

Chapter 2

Quantifying Soil Structure and Porosity Using Three-Dimensional Laser Scanning

Daniel R. Hirmas, Daniel Giménez, Edison A. Mome Filho,
Matthew Patterson, Kim Drager, Brian F. Platt and Dennis V. Eck

Abstract Advancements in three-dimensional (3D) digital surface scanning have opened up the possibility of capturing soil morphological information from irregular objects in high resolution. One of these advancements has been the development of a multistriple laser triangulation (MLT) technique that sweeps a series of laser stripes across a surface, while a camera offset from the laser source monitors the deformation and intensity of the reflected laser stripes. MLT scanning can be used to describe soil architecture (i.e., soil structure and porosity) from soil surfaces and soil specimens. The technique allows for the geometry of both small (<1 cm) and large (several meters) objects to be digitally captured in fine detail. In this paper, we provide examples of how MLT scanning has been applied to 3D soil specimens including the determination of bulk density from clods, the quantification of ped geometries, and the development of morphometrics from casted biopores. Examples of soil surface application of MLT scanning include the quantification of soil structure and interpedal pores from the field (excavation walls) and quantification of volume changes and crack formation in the laboratory

D.R. Hirmas (✉)

Department of Geography and Atmospheric Science, University of Kansas,
Lawrence, KS, USA
e-mail: hirmas@ku.edu

D. Giménez · M. Patterson

Department of Environmental Sciences, Rutgers University,
New Brunswick, NJ, USA

E.A. Mome Filho

Department of Soil Science, University of São Paulo, Piracicaba, SP, Brazil

K. Drager

Department of Animal Biology, University of Illinois, Urbana-Champaign,
Urbana, IL, USA

B.F. Platt

Department of Geology and Geological Engineering, University
of Mississippi, University, MS, USA

D.V. Eck

Bennett and Schulte Oil Company, Russell, KS, USA

(soil cores). When combined with other digital morphometric tools such as computed tomography, 3D laser scanning has the potential to quantify the architecture of soils across scales ranging from submicrometers to meters.

Keywords Soil structure • Quantitative pedology • Multistripe laser triangulation scanning • Soil macroporosity • Digital soil morphometrics

2.1 Introduction

Noncontact optical methods utilizing lasers to map the topography of fine-scale surfaces of soils have been developed and used in the study of soil roughness and surface deformation since the 1980s (e.g., Harral and Cove 1982; Huang and Bradford 1990; Eltz and Norton 1997; Darboux and Huang 2003; Zielinski et al. 2014). Most of these methods illuminate a spot on the soil surface that is detected by an optical sensor offset from the laser source, the distance from which is determined utilizing the geometry of the setup and the position of the spot on the detection array of the sensor (Thwaite and Bendeli 1980; Huang et al. 1988).

Laser scanners utilizing laser stripe triangulation techniques have recently been used in the investigation of soils, rocks, and sediments because of the ease of use, accuracy, portability, and low cost (e.g., Aguilar et al. 2009; Platt et al. 2010). These scanners project and sweep one or more laser stripes onto the surface of a target and generate a high-resolution three-dimensional (3D) surface based on the intensity of the laser stripes deformed on the surface of the object as observed from an image sensing array offset from the light source (Knighton et al. 2005; Usamentiaga et al. 2014). A 3D object is digitized when scans taken from multiple angles are aligned and merged into a continuous surface (Rossi et al. 2008).

Three-dimensional laser scanning opens up the possibility to digitize and, therefore, nondestructively measure both soil surfaces and 3D soil specimens (e.g., individual pedis). These techniques are well suited to quantify soil structure and the distribution of pores (i.e., soil architecture) of the soil profile. This is needed given the paucity of techniques available to quantify macroscale soil architecture despite its importance in pedological, hydrological, biological, physical, and chemical soil processes (Eck et al. 2013; Hartemink and Minasny 2014).

The objectives of this paper are to: (i) provide a relevant overview of the expanding literature on the application of 3D laser scanning techniques to quantify soil architecture; (ii) provide several examples of how this technology is being used; and (iii) guide future applications aimed at enhancing our understanding of soil morphology. Although other laser scanning methods have been employed in geosciences over the past three decades, we focus on multistripe laser triangulation (MLT) because of its high resolution and applicability of quantifying in situ interpedal macropores compared to noncontact spot methods.

2.2 Three-Dimensional MLT Scanning of Soils

2.2.1 Bulk Density

Bulk density is used in part to convert measurements of soil properties on a mass basis such as water content, soil organic carbon, NO_3^- -N, or calcium carbonate equivalent into a volumetric basis. Bulk density can be used in combination with soil texture as a predictor of soil hydraulic properties such as water retention and hydraulic conductivity (e.g., Schaap et al. 2001). Bulk density is used to calculate void ratio (i.e., ratio of pore volume to volume of the solids) and total porosity (i.e., a measure of the total volume fraction of pores in a soil). Total porosity is used as a measure of saturated volumetric water content and necessary to calculate degree of saturation in water retention measurements.

One of the first 3D applications of MLT scanning to soils was the accurate determination of bulk density from clods (Rossi et al. 2008). The clod method is the standard used by the USDA-NRCS when determining bulk density (Burt 2004) and is useful when the excavation of cores is impossible or impractical. For instance, in order to calculate the fine-earth bulk density of stony soils, the coarse fraction (>2 mm) has to be removed, weighed, and used to correct the total mass of the clod. Because the clod method is typically immersed in liquid saran or molten paraffin to make it water tight for volume determination by displacement using Archimedes' principle, separation of the coarse fraction can be problematic because the coating agent often binds the coarse and fine-earth fractions together (Hirmas and Furquim 2006). Thus, the determination of fine-earth bulk density from the clod method greatly benefits from a noninvasive procedure for obtaining clod volume.

The accurate determination of bulk density on very small (e.g., a few millimeters in diameter) and irregularly shaped samples such as soil aggregates is limited by the accuracy of the volume determination (Subroy et al. 2012). Several methods have been developed to measure these small samples, but they require sealing the aggregates by filling up the pores with an organic liquid and submerging the saturated aggregate in either the same liquid used to saturate the aggregate or in a liquid that is immiscible with it (Subroy et al. 2012).

Rossi et al. (2008) showed that the volumes obtained from the clod method (Blake and Hartge 1986) were not significantly different from those obtained by MLT scanning. Hirmas et al. (2013) compared aggregate volume measurements obtained with a displacement technique (Subroy et al. 2012) against those obtained by MLT scanning. They found no significant difference between the regression parameters. When data from those two studies are combined on the same plot, the measurements align close to the 1:1 line (Fig. 2.1), with a nearly perfect coefficient of determination ($r^2 = 0.999$). The axes in this figure are on a log scale to illustrate the 3-orders of magnitude in volumes provided by the combination of the traditional clod method and the aggregate displacement method, which indicates that MLT scanning can extend the range of volumes that a single method can measure. In theory, there is no upper limit for the scanner, provided there is enough storage and computational

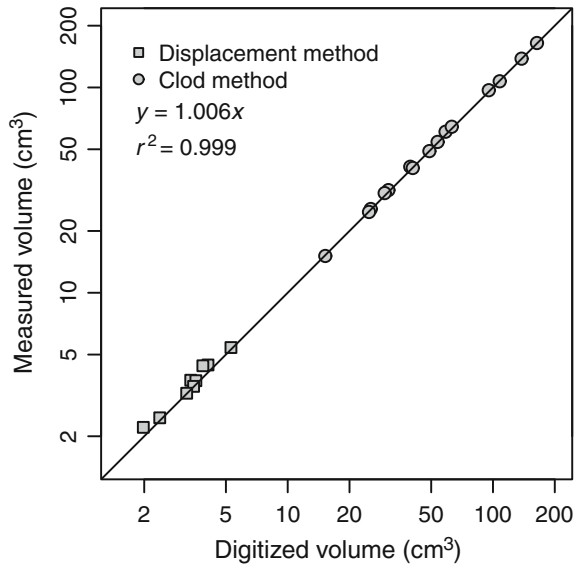


Fig. 2.1 Measured volume of aggregates and clods determined from a displacement technique (Subroy et al. 2012) and the clod method (Blake and Hartge 1986) against calculated volumes from MLT-derived digital scans. Data from Rossi et al. (2008) and Hirmas et al. (2013). The slope of the regression for a model where the y-intercept was set to zero and the coefficient of the determination are shown in the plot. *Solid line* represents a 1:1 relationship for reference

memory to process the resulting data. The lower limit is a function of the resolution of the scanner, which, for this study, was 120 μm (Desktop 3D Scanner Model 2020i, NextEngine, Inc., Santa Monica, CA) at its highest setting (macro).

Other methods for measuring bulk density such as the core method or excavation method (Blake and Hartge 1986) may also benefit from the incorporation of MLT scanning. The latter method is preferred where the loose consistence of a soil or the abundance of coarse fragments precludes the use of core or clod methods. In the excavation method, bulk density is obtained by excavating and weighing a dry quantity of soil and measuring the excavation volume (Blake and Hartge 1986). Variants of the excavation method primarily differ on the technique used to determine the volume of the cavity. Thus, there are two possible ways that this method could benefit from MLT scanning. First, the irregular surface of a cavity could be digitized in 3D by scanning the excavation surface before and after excavation of the material. This would allow for irregularities in the original surface of the excavation to be accounted for as opposed to current methods, which assume a previously leveled and smooth surface (Blake and Hartge 1986). Second, a modification of the excavation method proposes that casts of the cavity be made in dental plaster and volumes determined in the laboratory either by displacement or by MLT scanning (Frisbie et al. 2014). Drager (2014) used this plaster cast-MLT scanning modification of the excavation method to assess the effects of ant turbation on bulk density within a centimeter of excavated galleries in a fine-textured soil.

The determination of bulk density by MLT scanning is also applicable when bulk density is determined from core samples with an uneven soil surface, caused by, for example, gravel, roots, or soil shrinkage (see also Sect. 2.3.3). Accurate volume assessment is difficult in those situations due to the lack of a Euclidean shape.

Multistripe laser triangulation scanning has the potential to enhance analyses of soil architecture by allowing repeated bulk density measurements (i.e., at each soil water potential) on the same clod on which water retention is determined. This may be important in the volumetric determination of water content for water retention in swell and shrink soils (e.g., Vertisols).

2.2.2 *Quantification of Ped Geometries*

Rossi et al. (2008) showed that individual 3D peds could be digitized at high resolution and volumes measured accurately. New measurements of ped geometries and ped surface area can now be obtained from 3D laser scanning. Ped surface area, in particular, may prove useful in the quantification of ped type and grade or for assessing tortuosity of interpedal macropores. In addition, surface roughness may be quantified using an approach proposed by Platt et al. (2010) for characterizing irregular 3D target objects opening up possibilities to investigate the interface between inter- and intrapedal pores.

Figure 2.2a illustrates an individual prism specimen extracted from the soil and scanned using MLT. The ped is sliced in three orthogonal planes (Fig. 2.2b–d) to reveal cross sections and cutaways of the ped. These cross sections can be quantified from 2D measurements of size, shape, and orientation using standard image analysis software such as ImageJ (Research Services Branch, National Institute of Health, Bethesda, MD). Measurements of size include net, filled, and convex areas, equivalent area circular diameter, minimum circumscribed and maximum inscribed circle diameters, equivalent area ellipse major and minor axes lengths, caliper dimensions (i.e., Feret diameters; Fig. 2.2d), and perimeter (Russ 2011). Orientation measurements include the angle of the moment axis, longest caliper dimension, and major ellipse axis (Russ 2011). Common shape descriptors include form factor or circularity, roundness, aspect ratio, elongation, curl, convexity, solidity, compactness, modification ratio, and extent (Russ 2011). The possibility of quantifying ped shape is promising, as it is currently only characterized with subjective and categorical type classes (Schoeneberger et al. 2012). Quantifying shape can also be important when comparing ped or aggregate sizes from samples with different shapes (e.g., Hirmas et al. 2013).

2.2.3 *Biopore Morphometrics*

Biopores created from the movement of soil fauna and growth of soil flora have been digitized by MLT scanning and have allowed the quantification of biological

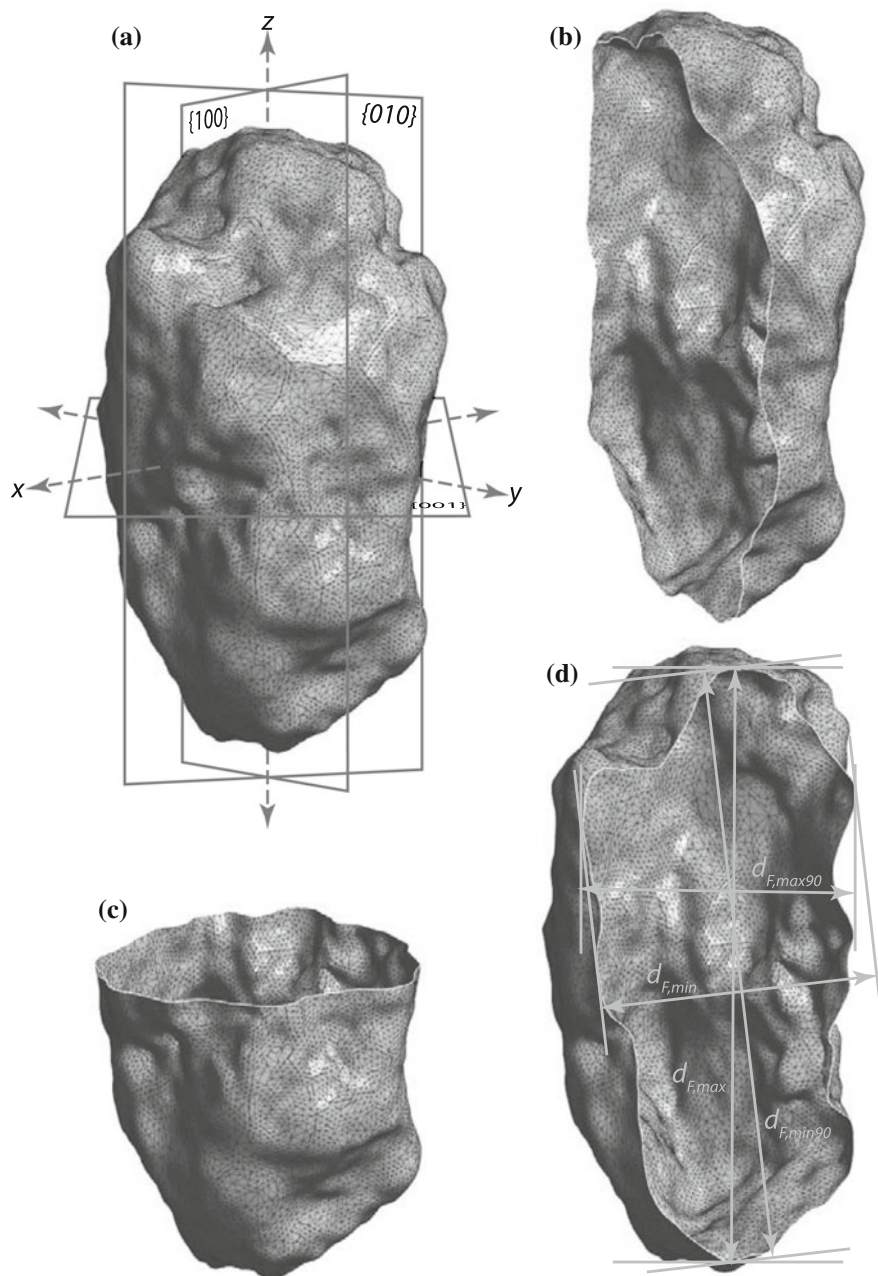


Fig. 2.2 a Scanned prismatic ped showing cross sections through the approximate middle of the aggregate and parallel to the b $\{100\}$ -plane, c $\{010\}$ -plane, and d $\{001\}$ -plane. Numbers between braces represent Miller index notation. Feret diameter calculations are shown in (d). Length of the ped along the z-axis in (a) is approximately 4.5 cm

macropore networks and identification of trace makers in paleosols for reconstruction of paleo-environments (Platt et al. 2010). These pores often represent complex and tortuous 3D geometries (Fig. 2.3a) and are typically casted with fiberglass, epoxy, plaster, wax, concrete or molten metal (Hasiotis and Bourke 2006; Tschinkel 2010); the casts are subsequently allowed to harden, excavated, and cleaned. The application of MLT scanning to these casted biopores will increase the accuracy of metrics such as lengths, diameters, and angles (Fig. 2.3); this is because pore measurements can be taken in the exact center of the digitized biopores avoiding errors with lengths measured on the outside of casted pores (Platt et al. 2010). Surface area of casted biopores can also be measured from MLT scans. The current method proposes to wrap the cast with a single layer of foil and record the foil weight. Surface area is then calculated from the known ratio of foil weight to surface area (Atkinson and Nash 1990).

Accurate determination of surface area from MLT scanning allows for the calculation of surface roughness over a range of scales (subcentimeter to meter). Platt et al. (2010) termed this measure surface area index and defined it as the ratio of the total surface area to the projected surface area of a biopore. The projected surface area is calculated as the surface area of a biopore after it has been smoothed;

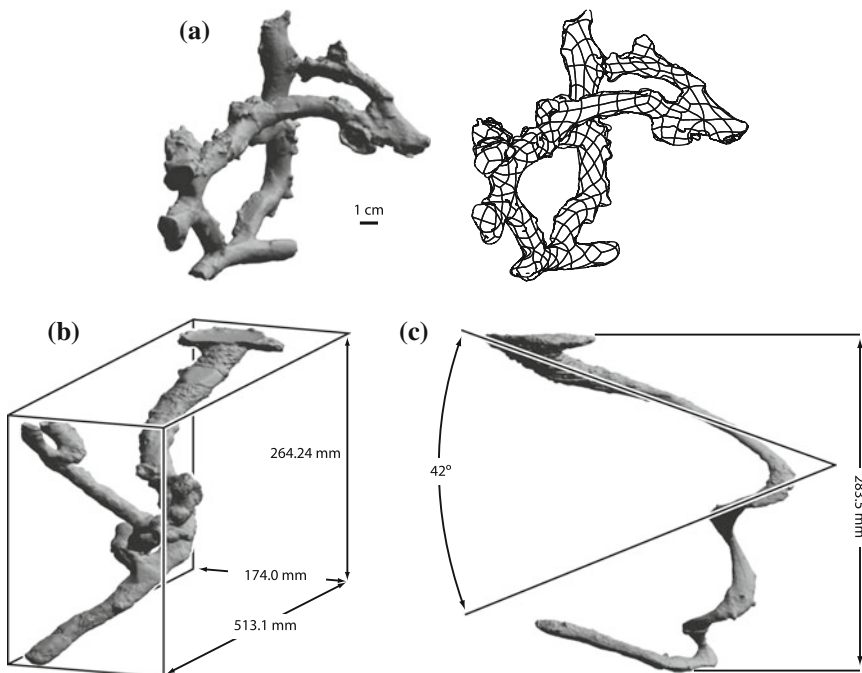


Fig. 2.3 Scanned resin casts of **a** an *Amphisbaena camurea* burrow alongside a smoothed mesh rendering of the cast, **b** desert skink (*Egernia inornata*) burrow with bounding box, and **c** a brown scorpion (*Urodacus* sp.) burrow showing depth and ramp angle of the uppermost spiral. Modified from Platt et al. (2010)

smoothing is attained by coarsening the resolution of the digital mesh, which effectively averages over the fine-scale variability. The resolution chosen to smooth the surface of the biopore represents the scale over which the surface roughness is calculated (Fig. 2.3a). Platt et al. (2010) plotted surface area index against mesh resolution for a variety of biopores and used the inflection point of the relationship to compare surface roughness of the casts. Results show that surface area index can be used to identify the trace makers of ichnological specimens.

Other metrics developed as a result of the MLT scanning of biopores include volume exploited (Fig. 2.3b)—defined as the ratio of volume of the biopore to volume of a bounding box fit around the biopore expressed as a percentage—and relative compactness—defined as the ratio of volume/surface area of the casted biopore to the volume/surface area of a sphere that has the same volume as the biopore (Platt et al. 2010). The relative compactness can be considered a measure of sphericity. The volume limitation of the scanner reached by Platt et al. (2010) that still preserved sufficient detail on the cast for ichnological interpretation was approximately 0.8 cm^3 .

2.2.4 Aggregate Mass–Volume Relationships

Soils commonly exhibit a hierarchical organization in the arrangement of primary particles where larger soil aggregates are formed from smaller and denser aggregates (Rieu and Sposito 1991; Hirmas et al. 2013). The inverse relationship in aggregate density and size stems from the “pore-exclusion principle,” which postulates that smaller aggregates selectively exclude larger interaggregate pores which increases their density compared to larger aggregates. This relationship can be described using a power-law relationship (Giménez et al. 2002):

$$M(d) = k_m d^{D_m} \quad (2.1)$$

where $M(d)$ is the aggregate mass, d is the diameter of the aggregate, k_m is the mass of an aggregate with unit diameter, and D_m is the slope of the relationship between $M(d)$ and d on a log–log plot also known as the fractal dimension of mass.

Previous attempts at examining the hierarchical organization in soils through the fractal dimension of mass have been restricted to relatively small aggregate sizes—often less than approximately 10 cm^3 . This is because it is difficult to measure the volume of larger aggregates or clods with the conventional methods (displacement techniques and/or clod method). Furthermore, as these methods either saturate the aggregates with an organic liquid or coat their outer surfaces, it has not been possible to investigate mass–volume relationships by sequentially breaking down large soil volumes into smaller aggregates while measuring volumes of the resulting fragments.

The ability for MLT scanning to nondestructively digitize aggregates down to approximately 1 cm^3 allows for the assessment of volumes over several orders of

magnitude using aggregates that were originally part of the same sample volume. For example, in a comparative study on the effects of tillage and erosion on the mass–volume relationship, Hirmas et al. (2013) investigated surface and subsurface horizons in two adjacent soils in northeastern Kansas. One of the soils was sampled in an unplowed native tallgrass prairie and the other in a restored field where erosion had exhumed the subsoil and a new shallow A horizon was forming in the previous Btss horizon. Six large ($\sim 1000 \text{ cm}^3$) clods were taken from each horizon investigated, weighed, scanned to measure volumes, and broken down into smaller aggregates that were weighed and scanned (Fig. 2.4a). This procedure was followed until MLT scanning was no longer practical and a displacement technique described by Subroy et al. (2012) was used for aggregates down to approximately 1 mm in diameter. As the shapes of the aggregates varied considerably, nine independent cross sections were digitally created for each aggregate and the roundness shape parameter was calculated, averaged, and used to normalize the diameter of each aggregate. The distribution of roots and organic carbon as controlled by the soil morphology had a considerable effect on the fractal distribution of mass in different aggregate size domains (Hirmas et al. 2013). The break point between aggregate size domains with different fractal dimensions of mass was controlled by the quantity of fines (silt + clay) and organic carbon in the soil. In addition, large within-horizon variability was observed in the k_m and D_m parameters from samples taken only centimeters to decimeters apart.

The study illustrated the usefulness of MLT scanning to investigate soil architecture at the horizon scale. Future MLT scanning should incorporate spatially explicit designs in the sampling of horizon-scale clods and aggregates to quantify the variability observed. In addition, the mass–volume approach would be enhanced if soil constituents were assessed on each aggregate from which size was determined. One possible way to achieve this is to couple MLT scanning with proximal

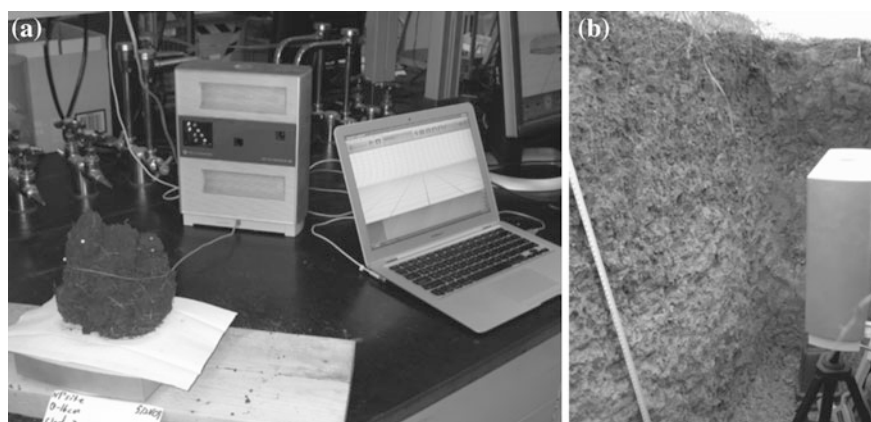


Fig. 2.4 Multistripe laser triangulation (MLT) scanner in use in the **a** laboratory scanning a large clod and **b** in the field scanning a prepared soil pit wall

sensing (e.g., hyperspectral scanning; Steffens and Buddenbaum 2013) to map binding agents such as organic matter or Fe-oxides on the surface of the aggregates.

2.3 Application of MLT Scanning for Digitizing Soil Surfaces

2.3.1 *Quantification of Soil Structure and Interpedal Pores from Excavation Walls*

An issue of MLT scanning is the formation of areas of missing data in the resulting digital mesh. These data gaps result from the offset between the laser source and the image sensing array in the triangulation arrangement. Sections of the laser stripes projected and swept on the surface disappear from the field of view of the camera as they are hidden in the recess of cracks.

Eck et al. (2013) took advantage of these data gaps to quantify interpedal macropores from an in situ soil excavation wall by projecting them onto a 2D surface and subsequently determining morphometrics using ImageJ (Fig. 2.4b). Several challenges were overcome in the process of surface scanning of the soil profile wall. First, the surface was prepared using a freeze and peel method following Hirmas (2013) to remove artifacts. Second, the surface was allowed to dry for several days in order to maximize the exposure of interpedal pores on the excavation wall. Third, scans were done at night to eliminate the effect of ambient light, minimize differences in surface color between horizons, and keep the scanner within its operational temperature range. Figure 2.5 illustrates a portion of a carefully prepared monolith surface that was saturated, allowed to dry, and scanned using MLT at various times during the drying process. The cracks became progressively more pronounced with time especially after 25 h of drying. The outlining of soil structural units such as angular blocks and prisms also became more striking as the soil surface dried (Fig. 2.5).

Size, shape, orientation, and abundance metrics were determined from the projected map of the surface scan gaps and included area, perimeter, bounding box width and height, ellipse axis lengths and angles, Feret diameters, circularity, roundness, pore density, pore fraction, and relative surface area (Eck et al. 2013). Probability distribution functions of these measurements within a depth zone can be assessed and used to create continuous depth functions of macropore interpedal geometries and quantify the uncertainty of these properties. Several of these metrics correlated well to traditional descriptions of the grade, size, and type of soil structure following Schoeneberger et al. (2012). The pore width obtained from MLT scanning in combination with coefficient of linear extensibility measurements can be used to predict the effective saturated hydraulic conductivity of the soil (Eck et al. 2016).

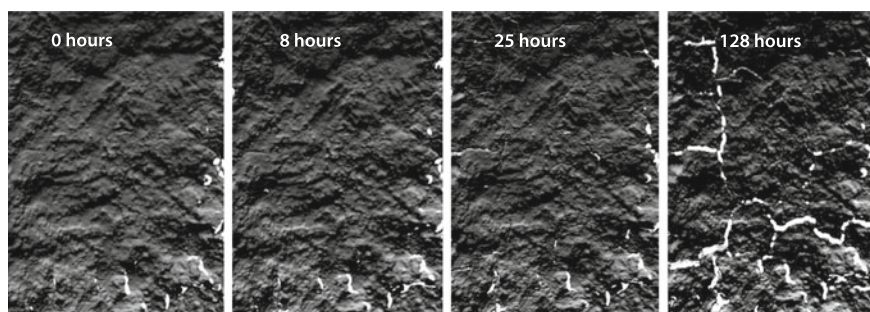


Fig. 2.5 Scanned monolith at 0, 8, 25, and 128 h after prolonged visible saturation of the profile surface. Depths are from 38 to 61 cm below the soil surface. *White areas* in the sections are data not returned during the MLT scan and represent pores outlining structural units in the digital mesh

The ability to quantify interpedal macropore geometries and soil structure in the field from a soil profile represents a step forward in understanding the genesis of soil architecture and its interactions with hydrological and transport processes. As with quantifying aggregate mass–volume relationships, quantifying and mapping the spatial arrangement of macropores and soil structure would be enhanced if coupled to high-resolution proximal sensing techniques. Here, the movement of soil constituents such as clay and organic matter and the presence of redoximorphic features could be consistently and quantitatively assessed in relation to soil structure and proximity to macropores. This ability would aid the hydrological interpretation of a site and likely enhance and standardize the assessment of soil quality.

2.3.2 *Geostatistical and Multifractal Analyses of Soil Surfaces*

Surface roughness is the result of the structural organization of the soil at the surface and is influenced by both extrinsic (e.g., tillage and topography) and intrinsic (e.g., texture and aggregate size distribution) factors. Surface information from MLT makes it possible to generate high-resolution (≤ 1 mm) digital elevation models (DEMs; Fig. 2.6) suited to investigate intrinsic factors defining microtopography, such as the mapping of clods on freshly tilled surfaces (Chimi-Chiadjeu et al. 2014).

Surface roughness is characterized by the statistical distribution of elevations either considering or disregarding their spatial location. The semivariogram (Dalla Rosa et al. 2012) and related fractal techniques (Huang and Bradford 1992; Vidal Vázquez et al. 2005) are examples of considering spatial location. Multifractal studies of soil surface elevations have been conducted, however, disregarding the spatial location of the elevation points (García Moreno et al. 2008; San José Martínez et al. 2009). Multifractal models consider the distribution of elevations as

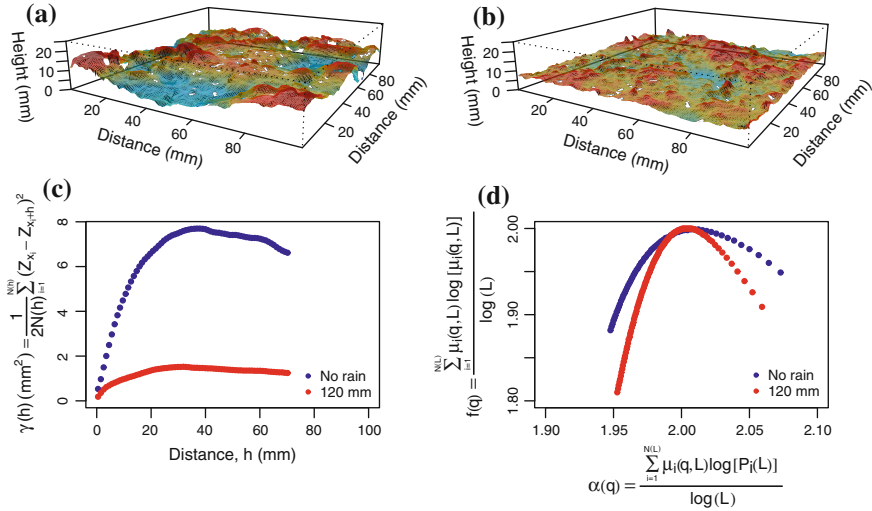


Fig. 2.6 Surface digital elevation models (DEMs) with a resolution of $500 \mu\text{m}^2$ obtained in the laboratory from the center ($10 \times 10 \text{ cm}^2$) of soil blocks collected **a** immediately after tillage (heavy disk + leveling harrow), and **b** after the application of 120 mm of simulated rainfall during a 1-h period, and the corresponding **c** semivariograms and **d** multifractal spectra estimated from the distribution of elevations. The experiment was located at the campus of the Luiz de Queiroz College of Agriculture of the University of São Paulo in Piracicaba, Brazil. The soils are classified as Rhodic Kandiudalfs. White areas are data gaps in the MLT mesh

probabilities, P_i , and use it to calculate the partition function $\mu_i(q, L)$ (Chhabra and Jensen 1989):

$$\mu_i(q, L) = \frac{P_i(L)^q}{\sum_{i=1}^{N(L)} P_i^q} \quad (2.2)$$

where L defines the scale and q the moments of the measure. The main expression of a multifractal system is its $f(\alpha)$ spectrum, which represents the relationship between the exponent α that characterizes the local behavior of $P_i(L)$ and its fractal dimension $f(\alpha)$, both calculated using the partition function (Fig. 2.6).

Figure 2.6 shows DEMs of soil blocks ($10 \times 10 \text{ cm}$) sampled from a freshly tilled soil and after 120 mm of rainfall. Multifractal spectra were calculated according to Posadas et al. (2003) with the software Multifractal Analysis System 3.0 (<http://inrm.cip.cgiar.org/home/downmod.htm>, accessed on June 27, 2015) after rasterizing the MLT data. Semivariograms were calculated using the geoR package (Ribeiro and Diggle 2015). Both the semivariogram and multifractal spectra were sensitive to changes in the surface properties induced by rainfall. Rainfall reduced the variation of elevation values as reflected by a decrease in the sill of the semivariograms and by a narrower range of α values in the multifractal spectra. The disadvantage of the MLT method to generate surface elevations is the presence of

data gaps (Fig. 2.6) that could compromise the multifractal analysis. This problem can be avoided by using techniques that do not define L by averaging increasingly larger surfaces, but rather by considering L as the separation between elevation points (Davis et al. 1994).

2.3.3 Soil Shrinkage and Volume Determination

In the investigation of soil surface deformation from shrinkage, laser triangulation scanning has been useful in accurately assessing processes such as curling (e.g., Zielinski et al. 2014) and crack formation dynamics (e.g., Sanchez et al. 2013). In these investigations, it is important that the surface be prepared to maintain the features under consideration. Figure 2.7 illustrates a surface that was prepared with the freeze and peel method (Hirmas 2013) leaving behind an irregular micro-topography. Using the edge of the core as a reference, the surface of the core was digitized by MLT and the missing volume determined to be 16.2 cm^3 which was 6.4 % of the core volume.

Soil shrinkage during desiccation has been studied using MLT (Sanchez et al. 2013). Volume changes were quantified as well as the dynamics of crack formation at the surfaces of packed cores along with soil water content (estimated by recording the loss of mass of the cores). By combining the morphological characterization of the surface with soil water content, this approach allows the development of mechanistic models of the evaporation process. Figure 2.8a shows results of a similar experiment using a soil core sampled from the argillic (2Bt3)

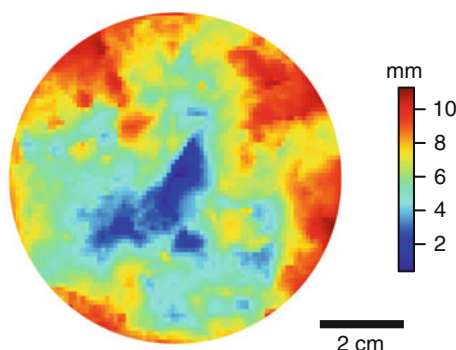


Fig. 2.7 A MLT-derived digital elevation model (DEM) of the surface of an approximately 250 cm^3 core (8 cm diameter \times 5 cm length) sampled from the National Ecological Observatory Network (NEON) Konza Prairie Biological Station Relocatable site for bulk density, hydraulic conductivity, and water retention determination. The exposed surface of the core was prepared using a freeze and peel following Hirmas (2013) leaving behind a smear-free but irregular surface. The volume between the end of the core ring and the irregular surface was calculated as 16.2 cm^3 representing 6.4 % of the total volume of the core

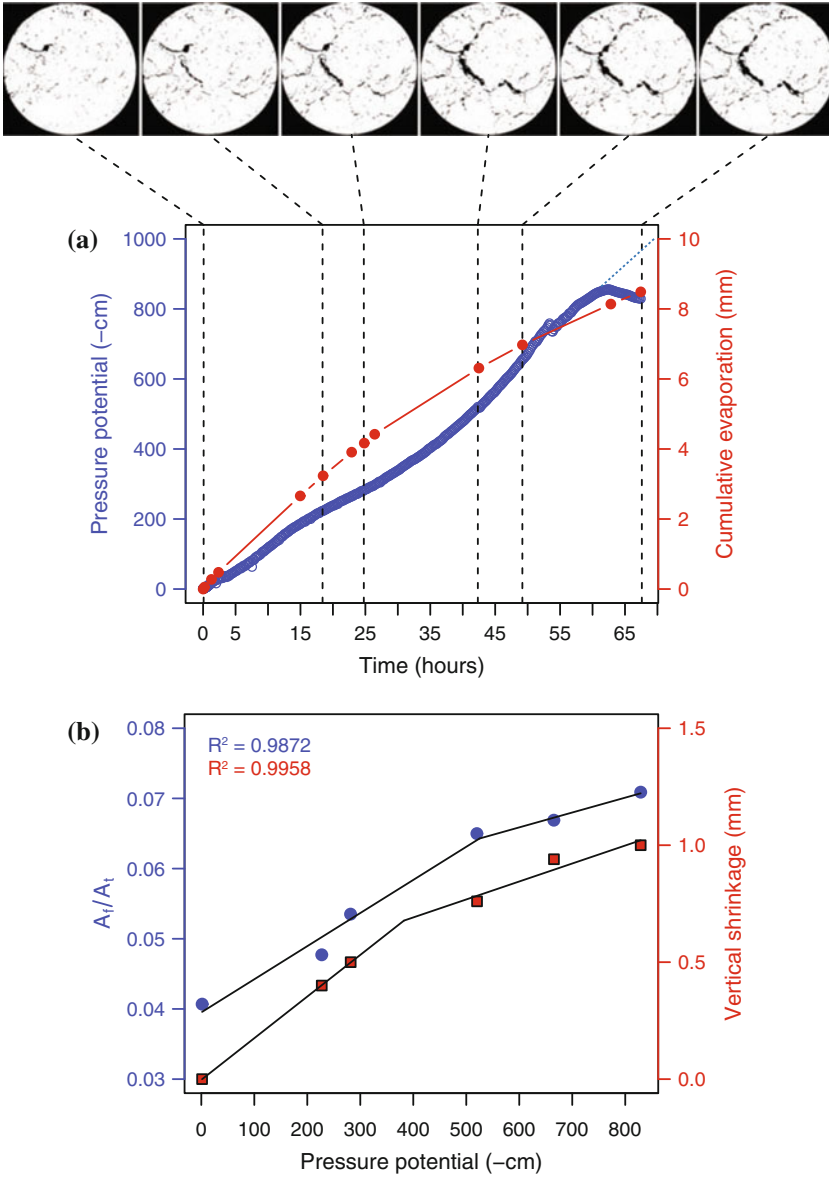


Fig. 2.8 **a** Pressure potential and cumulative evaporation measurements as a function of time from an evaporation experiment. Pressure potential was measured using a tensiometer located at 3.75 cm depth in a cylindrical 8 cm diameter \times 5 cm height core. The tensiometer failed at approximately –800 cm. *Blue dotted line* is the projected pressure potential. Binary images (*top*) are taken from MLT scans performed at times indicated by the *black dashed lines*. **b** Lateral and vertical shrinkage trends. The lines are piecewise regression fits between soil pressure potential and fracture areas from image analysis, A_f , normalized by the total surface area of soil, A_t (*blue*), and between pressure potential and mean vertical shrinkage (*red*)

horizon of a fine, smectitic, mesic Pachic Argiudoll (Rosendale series). The core was water-saturated and allowed to dry by evaporation. Water loss was measured by frequently weighing the core, and pressure potential was recorded throughout the duration of the experiment with a tensiometer placed 3.75 cm below the surface. Similar to Eck et al. (2013), the area covered by the cracks was mapped with MLT six times and the results quantified with ImageJ. The nonlinear nature of the evaporation process can be seen at pressure potentials between -400 and -500 cm where the rate of drying determined with the tensiometer increased, while the evaporation rate declined. The evaporation rate decreased despite the increase in evaporating surface area created by the continuous formation of cracks until the end of the experiment (Fig. 2.8a). The MLT data allowed for comparison between the rates of crack formation (lateral shrinkage) and vertical shrinkage, estimated as the average reduction in sample height within the core (see Fig. 2.7). For this sample, a similar rate was observed in both directions (Fig. 2.8b), suggesting an isotropic process. High-resolution MLT scanning can be used to increase our understanding of evaporation processes in soils using both the elevation data returned from the scanner as well as the gaps in the digital mesh that can be used to map and quantify the patterns and abundance of cracks.

2.4 Conclusions and Future Directions

Digital morphometrics is defined by Hartemink and Minasny (2014) as the, "... application of tools and techniques for measuring and quantifying soil profile attributes and deriving continuous depth functions." To the growing list of tools and techniques, we add laser stripe scanning technology as a means of quantifying soil architecture, which has proven to be one of the most elusive soil profile attributes for which to quantify and derive continuous depth functions. In particular, MLT scanning can be used to quantify the spatial arrangement of soil particles and pores at scales ranging from centimeters to meters (i.e., horizon to pedon scales). As MLT is a surface scanning technique with no depth penetration and because constituent information is not obtained about the surface being scanned, a coupled approach using this scanning in combination with proximal sensing such as hyperspectral scanning and fine-scale geophysical imaging with X-ray CT holds potential to advance our understanding of soil morphology.

Other 3D digitizing methods such as time-of-flight scanning, structured-light scanning, photogrammetry, and silhouette techniques have been used to digitize and measure a variety of soil properties. We expect that most of the concepts discussed in this paper will be equally applicable to these techniques in the investigation of soil architecture.

References

- Aguilar MA, Aguilar FJ, Negreiros J (2009) Off-the-shelf laser scanning and close-range digital photogrammetry for measuring agricultural soils microrelief. *Biosyst Eng* 103:504–517
- Atkinson RJA, Nash RDM (1990) Some preliminary observations on the burrows of *Callianassa subterranea* (Montagu) (Decapoda: Thalassinidea) from the west coast of Scotland. *J Nat Hist* 24:403–413
- Blake GR, Hartge KH (1986) Bulk density. In: Klute A (ed) *Methods of soil analysis*, Part 1, 2nd edn. Agron. Monogr. 9. ASA and SSSA, Madison, WI, pp 363–375
- Burt R (ed) (2004) *Soil survey laboratory methods manual*, Ver. 4.0, Soil Survey Investigations Report No. 42. Natural Resources Conservation Service, Washington, DC
- Chhabra AB, Jensen RV (1989) Direct determination of the f (alpha) singularity spectrum. *Phys Rev Lett* 62–12:1327–1330
- Chimi-Chiadjeu O, Hégarat-Masclé S, Vannier E, Taconet O, Dusséaux R (2014) Automatic clod detection and boundary estimation from Digital Elevation Model images using different approaches. *Catena* 118:73–83
- Dalla Rosa J, Cooper M, Darboux F, Medeiros JC (2012) Soil roughness evolution in different tillage systems under simulated rainfall using a semivariogram-based index. *Soil Tillage Res* 124:226–232
- Darboux F, Huang C (2003) An instantaneous-profile laser scanner to measure soil surface microtopography. *Soil Sci Soc Am J* 67:92–99
- Davis A, Marshak A, Wiscombe W, Cahalan R (1994) Multifractal characterizations of nonstationarity and intermittency in geophysical fields—Observed, retrieved, or simulated. *J Geophys Res Atmos* 99:8055–8072
- Drager K (2014) Alterations of fine and coarse-textured soil material caused by the ant *Formica subsericea*. MS thesis. University of Kansas, Lawrence, KS
- Eck DV, Hirmas DR, Giménez D (2013) Quantifying soil structure from field excavation walls using multistripe laser triangulation scanning. *Soil Sci Soc Am J* 77:1319–1328
- Eck DV, Qin M, Hirmas DR, Giménez D, Brunsell N (2016) Relating quantitative soil structure metrics to saturated hydraulic conductivity. *Vadose Zone J* doi: [10.2136/vzj2015.05.0083](https://doi.org/10.2136/vzj2015.05.0083)
- Eltz FLF, Norton LD (1997) Surface roughness changes as affected by rainfall erosivity, tillage, and canopy cover. *Soil Sci Soc Am J* 61:1746–1755
- Frisbie JA, Graham RC, Lee BD (2014) A plaster cast method for determining soil bulk density. *Soil Sci* 179:103–106
- García Moreno R, Díaz Álvarez M, Saa Requejo CA, Tarquis AM (2008) Multifractal analysis of soil surface roughness. *Vadose Zone J* 7-2:512–520
- Giménez D, Karmon JL, Posadas A, Shaw RK (2002) Fractal dimensions of mass estimated from intact and eroded soil aggregates. *Soil Tillage Res* 64:165–172
- Harral BB, Cove CA (1982) Development of an optical displacement transducer for the measurement of soil surface profiles. *J Soil Agric Eng Res* 27:412–429
- Hartemink AE, Minasny B (2014) Towards digital soil morphometrics. *Geoderma* 230–231:305–317
- Hasiotis ST, Bourke MC (2006) Continental trace fossils and museum exhibits: displaying organism behavior frozen in time. *Geol Curator* 8:211–226
- Hirmas DR (2013) A simple method for removing artifacts from moist fine-textured soil faces 77:591–593
- Hirmas DR, Furquim SAC (2006) Simple modification of the clod method for determining bulk density of very gravelly soils. *Commun Soil Sci Plant Anal* 37:899–906
- Hirmas DR, Giménez D, Subroy V, Platt BF (2013) Fractal distribution of mass from the millimeter- to decimeter-scale in two soils under native and restored tallgrass prairie. *Geoderma* 207–208:121–130
- Huang C, Bradford JM (1990) Portable laser scanner for measuring soil surface roughness. *Soil Sci Soc Am J* 54:1402–1406

- Huang C, Bradford JM (1992) Applications of a laser scanner to quantify soil microtopography. *Soil Sci Soc Am J* 56:14–21
- Huang C, White I, Thwaite EG, Bendeli A (1988) A noncontact laser system for measuring soil surface topography. *Soil Sci Soc Am J* 52:350–355
- Knighton MS, Agabra DS, McKinley WD, Zheng JZ, Drobnis DD, Logan JD, Bahhour BF, Haynie JE, Vuong KH, Tandon A, Sidney KE, Diaconescu PL (2005) Three dimensional digitizer using multiple methods. US Patent 6,980,302 B2. Filed 17 Sept 2003, issued 27 Dec 2005
- Platt BF, Hasiotis ST, Hirmas DR (2010) Use of low-cost multistripe laser triangulation (MLT) scanning technology for three-dimensional, quantitative paleoichnological and neoichnological studies. *J Sedim Res* 80:590–610
- Posadas A, Giménez D, Quiroz R, Protz R (2003) Multifractal characterization of soil pore systems. *Soil Sci Soc Am J* 67:1361–1369
- Ribeiro Jr PJ, Diggle PJ (2015) *geoR: analysis of geostatistical data*. R package version 1.7-5.1. <http://CRAN.R-project.org/package=geoR>
- Rieu M, Sposito G (1991) Fractal fragmentation, soil porosity, and soil-water properties. I. Theory. *Soil Sci Soc Am J* 55:1231–1238
- Rossi AM, Hirmas DR, Graham RC, Sternberg PD (2008) Bulk density determination by automated three-dimensional laser scanning. *Soil Sci Soc Am J* 72:1591–1593
- Russ JC (2011) *The image processing handbook*, 6th edn. CRC Press, Boca Raton
- Sanchez M, Atique A, Kim S, Romero E, Zielinski M (2013) Exploring desiccation cracks in soils using a 2D profile laser device. *Acta Geotech* 8:583–596
- San José Martínez F, Caniego J, Guber A, Pachepsky Y, Reyes M (2009) Multifractal modeling of soil microtopography with multiple transects data. *Ecol Complexity* 6:240–245
- Schaap MG, Leij FJ, van Genuchten MTh (2001) ROSETTA: a computer program for estimating soil hydraulic parameters with hierarchical pedotransfer functions. *J Hydrol* 251:163–176
- Schoeneberger PJ, Wysocki DA, Benham EC, Soil Survey Staff (2012) *Field book for describing and sampling soils*, ver. 3.0. Natural Resources Conservation Service, National Soil Survey Center, Lincoln, NE
- Steffens M, Buddenbaum H (2013) Laboratory imaging spectroscopy of a stagnic Luvisol profile —High resolution soil characterisation, classification and mapping of elemental concentrations. *Geoderma* 195–196:122–132
- Subroy V, Giménez D, Hirmas DR, Takhistov P (2012) On determining soil aggregate bulk density by displacement in two immiscible liquids. *Soil Sci Soc Am J* 76:1212–1216
- Thwaite EG, Bendeli A (1980) A noncontact profile recording instrument. In: *Proceedings of the international conference on manufacturing engineering*, Melbourne, Australia, 25–27 Aug 1980. Institution of Engineers in Canberra, ACT, Australia, pp 393–396
- Tschinkel WR (2010) Methods for casting subterranean ant nests. *J Insect Sci* 10:88
- Usamentiaga R, Molleda J, Garcia DF, Bulnes FG (2014) Removing vibrations in 3D reconstruction using multiple laser stripes. *Opt Lasers Eng* 53:51–59
- Vidal Vázquez E, Vivas-Miranda JG, Paz González A (2005) Characterizing anisotropy and heterogeneity of soil surface microtopography using fractal models. *Ecol Model* 182:337–353
- Zielinski M, Sánchez M, Romero E, Atique A (2014) Precise observation of soil surface curling. *Geoderma* 226–227:85–93

<http://www.springer.com/978-3-319-28294-7>

Digital Soil Morphometrics

Hartemink, A.E.; Minasny, B. (Eds.)

2016, XVII, 442 p. 177 illus., 122 illus. in color.,

Hardcover

ISBN: 978-3-319-28294-7